Virus-Plant Protein Interactions: The Importance of the *Potato leafroll virus* Readthrough Protein

Honors Thesis
Presented to the College of Agriculture and Life Sciences, Plant Science
of Cornell University
in Partial Fulfillment of the Requirements for the
Research Honors Program

by
Jaclyn Elizabeth Mahoney
May 2013

Dr. Michelle Cilia

Abstract

Potato leafroll virus' (PLRV's) C-terminal domain of the readthrough protein (RTP) is known to be involved with active retention of the virus in plant phloem. In this investigative study we used a combined proteomics and molecular virology approach to determine the identity and function of those plant proteins that are interacting with the readthrough domain of the RTP. Using a novel, on-plate co-immunoprecipitation method, we compared those plant proteins co-immunoprecipitating with the wild type form of PLRV with those that co-immunoprecipitate with a mutant form of the virus lacking the readthrough domain using *N. benthamiana* as a model system. Controls were thoroughly characterized to identify proteins that were non-specifically interacting with virus. Our research yielded four candidate proteins that appear to interact with the readthrough domain of the RTP and hence, are likely involved with phloem retention. The candidate proteins are as follows: 14-3-3 protein (AT1G78300.1), probable 26S proteasome non-ATPase regulatory subunit 3, membrane steroid-binding protein 2, and elicitor-inducible protein EIG J7. These four proteins were detected in the WT PLRV infected *N. benthamiana* as having 2.5-fold or greater enrichment as judged by spectral counts over a mutant that lacked the readthrough domain (ΔRTP) or control *N. benthamiana* tissue, and were also found in the host potato system with 2.5-fold or greater enrichment in WT PLRV infected potato as compared to healthy potato. These candidate proteins will be the focus of future validation studies to determine the function of these plant proteins in PLRV infection.

Introduction

Potato leafroll virus (PLRV), is a member of the genus *Polerovirus* in the family *Luteoviridae* that infects potato crops worldwide, causing economic hardships and devastating

staple crop losses. The virus is vectored most efficiently by the aphid *Myzus persicae* in a circulative-persistent manner, where the virus must pass through the midgut into the haemolymph and then across the accessory salivary glands to be transmitted to plants (Gray and Banerjee 1999; Gray and Gildow 2003). Once deposited in the plant by a feeding aphid, PLRV movement remains restricted to the phloem tissues (Peter et al. 2009). Current disease management strategies are limited to cultural measures including the prophylactic use of insecticides to control aphid vectors. However, this method is often ineffective and environmentally harmful. By studying the protein interactions of PLRV within plants, we will further our understanding of what host proteins are interacting with the virus. These advances in knowledge will ultimately help with the design of improved and safe strategies to control virus infection.

PLRV has a single stranded, positive sense RNA genome that is packaged in an icosohedral shaped capsid comprised of two structural proteins (Fig.1). The coat protein (CP) encoded by ORF 3, makes up the majority of the capsid while a minor amount is made up of the readthrough protein (RTP), which is translated via a leaky stop codon in the CP ORF (Fig.1) (Bahner et al. 1990). The RTP is not required for particle assembly or plant infection, but particles containing only the CP are not transmissible by aphids to plants (Mohan et al. 1995; Chay et al. 1996; Peter et al. 2008). Both proteins regulate virus movement in plants. The CP is required for local and systemic movement; the RTP acts *in trans* to retain virus in the phloem where it is available to aphids, and has co-lateral effects on transmission (Peter et al. 2009). How these two virus proteins regulate the different activities in plants is unknown, but we hypothesize that virions regulate these activities via interactions with host proteins. With a genome that only encodes for seven viral proteins, protein-protein interactions with its host may help to provide

93 PLRV with the biochemical flexibility to move throughout the plant in a way that promotes
94 efficient acquisition by its aphid vector.
95 Plant cells are connected by cytoplasmic channels called plasmodesmata (PDs) that allow
96 the transfer of nutrients and signals necessary for growth and development (Cilia et al. 2002;
97 Cilia and Jackson 2004). PDs transverse the cell walls of neighboring cells. Akin to nuclear
98 pores, molecules are thought to traffic through the cytoplasmic channels either by a non-targeted
99 or passive mechanism, if they are under the size exclusion limit of the pore, or by a selective and
100 regulated mechanism, if they possess an intrinsic trafficking signal(s). Plant viruses fall into the
101 latter category and have been hypothesized to hijack existing cell-to-cell transport pathways for
102 local and systemic virus movement within the plant (Cilia et al. 2002; Cilia and Jackson 2004).
103 The different mechanisms of transport through PD are well reviewed (Cilia and Jackson 2004;
104 Benitez-Alfonso et al. 2010; Burch-Smith et al. 2011; Maule et al. 2011; Ritzenthaler 2011;
105 Schoelz et al. 2011; Ueki and Citovsky 2011; Burch-Smith and Zambryski 2012; Marin-
106 Gonzalez and Suarez-Lopez 2012), however these current models are limited in explaining how
107 insect transmitted viruses, like PLRV, move systemically as assembled virion and not as
108 ribonulear protein complexes as seen for other plant virus like TMV (Liu and Nelson 2013).
109 The central dogma for plant virus cell-to-cell movement is that all land plant virus
110 genomes encode a cell-to-cell movement protein. A primary function of the movement protein is
111 to aid in the transport of the virus genome from cell to cell via interactions with host factors
112 (Ueki and Citovsky 2011). Until recently, it was presumed that luteovirids did not encode a true
113 movement protein, and thus these viruses remained trapped in the phloem tissues. Recently the
114 Gray lab showed that phloem retention of luteovirids was an active strategy mediated by the C-
115 terminal domain of the RTP (Peter et al. 2009). Whereas wild type (WT) virus remains inside

the phloem during infection, deletion of the RTP C-terminal domain permits the virus to efficiently move out of the phloem and infect mesophyll tissues. This is mediated by the trans-form (not incorporated into virions) of the RTP (Peter et al. 2009). Aphids cannot acquire virus directly from plants infected with the RTP C-terminal deletion mutant; however, if virus is purified from these plants and fed to aphids using Parafilm membrane sachets, the virus is transmitted indicating that virus acquisition by aphids is dependent on virus localization-specific effects (Peter et al. 2009).

There are a number of methods to investigate the molecular pathways that viruses use to infect plants. Traditional methods use yeast two hybrid or co-localizations with fluorescently tagged proteins. However, these methods are limited in scope because only one interaction can be examined at a time. A new approach was developed by Cristea and Chait (Cristea and Chait 2011), that involved co-immunoprecipitation (co-IP) coupled with nanoflow liquid chromatography coupled to tandem mass spectrometry (nLC-MS/MS) to discover the virus-host protein interactome, that is a description of the viral proteins interacting directly or in complex with many host proteins (Cristea and Chait 2011). Using this method, the virus-host interactions can be studied on a proteome-wide scale, and can be detected as they exist in native conditions, not under denaturing conditions or in a non-host plant such as in yeast.

The work presented here focused on a biochemical characterization of virion and RTP-plant protein interactomes, e.g., the proteins that may interact with PLRV virions and/or the RTP. Using co-IP coupled to nLC-MS/MS, the PLRV-plant interactome in a model host, *N. benthamiana*, and a natural host, potato (*S. tuberosum*) was studied. We co-immunoprecipitated virus-plant protein complexes from plant tissue and used nLC-MS/MS to identify the interacting proteins. Using genome-specific protein databases and label-free quantification based on spectral

counts, we identified a number of proteins shared in the two hosts and more importantly, 87 that were unique to systemically-infected potato (natural infection). We also found 7 proteins enriched in both WT PLRV *N. benthamiana* and WT PLRV infected potato co-IPs over mock or mutant PLRV, 4 of which have 2.5-fold or greater enrichment, and will be the focus of future study. Notably, we coupled molecular virology to co-IP-LC-MS/MS to reveal plant proteins that putatively interact in the RTP.

Materials and Methods

Agrobacterium-mediated transformation of *N. benthamiana*

Agroinfiltration into *N. benthamiana* mesophyll cells was carried out using *Agrobacterium tumefaciens* (LB4404) cultures containing the full-length infectious clone of WT PLRV (Canadian isolate) and ΔRTP mutant (Kaplan et al. 2007) as described below:

5 mL cultures of LB (lysogeny broth) medium supplemented with kanamyacin (50ug/mL) and MgSO4 (0.2g/mL) were inoculated with a single colony of LB4404 *A. tumefaciens* transformed with infectious wild-type (WT) and mutant PLRV and incubated overnight at 28°C, with shaking at 250 revolutions per minute (rpm). A 5 mL culture of LB containing MgSO4 without antibiotics was inoculated with LB4404 as a mock control. Cultures were then used to inoculate 200 mL of LB supplemented with kanamyacin (50ug/mL), rifampicin (25ug/mL), 20 uM acetosyringone and MgSO4 (0.2g/mL) for the PLRV infectious clones and LB supplemented with rifampicin (25ug/mL), 20 uM Acetosyringone and MgSO4 (0.2g/mL) for LB4404 mock control. Cultures were incubated over-night at 28°C, shaking at 250 rpms, and cells were pelleted by centrifugation at 6000 rpm for 15 min using a JA-14 Beckman rotor. Pellets were resuspended in a solution containing 10 mM MgCl2, 10 mM 2-(*N*-

morpholio)ethanesulfonic acid (MES), and 100uM acetosyringone (re-suspension buffer) and incubated at room temperature for at least 2 hr. The cell density of culture samples was measured using optical density at 600 nm. This information was used to calculate the volumes of dilution for individual cultures to ensure equal cell density when inoculating plant samples. Samples with OD600 between 0.4 and 1.0 were diluted with re-suspension buffer to an OD600 between 0.3 and 0.4 for infiltration into *N. benthamiana* leaves.

N. benthamiana plants were reared from seeds from the Martin Lab (Boyce Thompson Institute, Ithaca, NY. Plants were grown for three to four weeks in a greenhouse at 25°C and a 12 hr photoperiod. Using 5cc insulin syringes without needles, leaves were infiltrated with the re-suspended agrobacterium samples following a standard infiltration protocol. Briefly, cultures were delivered into plant tissues by pressing the syringe containing the bacterial culture to the underside of leaves, and providing counter-pressure with a finger on the other side. Four leaves per plant, on average, were successfully infiltrated. Leaves with fewer veins worked best, and cotyledons were avoided. Those *N. benthamiana* plants expressing discoloration or symptoms of disease were not used for experimentation. *N. benthamiana* plants were difficult to infiltrate at midday or those days when temperatures were high, as we hypothesized that stomatal pore openings were restricted. If needed, small holes were initially made in the underside of the leaf with needles or toothpicks to ease infiltration. We found that optimal temperature for *Agrobacterium* mediated transformation of *N. benthamiana* leaves is between 22-25°C. Approximately 30-60g of leaf tissue was harvested 3-4 d post agro-infiltration and placed in labeled freezer bags. Tissue was stored at -80°C until used.

Systemic infection of *S. tuberosum*

Nonviruliferous *Myzus persicae* aphids were allowed a 48 hr acquisition period on leaf tissue collected from *S. tuberosum* plants naturally infected with a Michigan strain of PLRV growing in a Florida field during the winter of 2009. These aphids were then transferred to *S. tuberosum* cultivars NY 129 and Russet Burbank grown in greenhouse conditions for a 48 hr inoculation period. Systemically infected RB and NY129 plants were used as source plants for several rounds of aphid transmission to new RB and NY129 plantlets. The tubers developed from these systemically infected plants were collected and stored at 4°C. *S. tuberosum* plants used in this study were grown from these tubers.

Double antibody sandwich enzyme-linked immunosorbent assay

Double antibody sandwich enzyme-linked immunosorbent assay (DAS-ELISA) was used to quantify the virus titer in agro-infiltrated *N. benthamiana* and naturally infected *S. tuberosum* leaves. Tissue punches from infected leaves were collected and used as samples for the DAS-ELISAs. Healthy negative and PLRV infected positive controls were also collected and used for comparison. Collected tissue samples were put in microcentrifuge tubes with 150 microlitres of 1X PBS buffer and manually crushed with wooden rods. ELISA plates were prepared and loaded as follows: The 96-well plates were first coated with 100 ul per well of Agdia (Elkhart, IN) anti-PLRV capture antibody diluted 1:200 in the coating buffer (15 mM Na_2CO_3, 35 mM $NaHCO_3$) and allowed to incubate for 2 hrs at 37°C. Plates were washed 3 times with 1X PBS- 0.5% tween. 100 microlitres of the *Agrobacterium*-infiltrated *N. benthamiana* homogenate samples were added per well and plates were incubated overnight at 4°C. Plates were again washed three times with 1X PBS- 5% tween. Agdia anti-PLRV detection antibody conjugated with alkaline phosphatase was diluted 1:200 in 1X PBS + 0.4% Nonfat dry milk. 100 ul was added per well,

and the plates incubated 2 hrs at 37°C. Finally, the DAS-ELISA plates were washed as described above and 100 microlitres of the substrate buffer supplemented with Agdia PNP Alkaline phosphatase substrate tablets (1 tablet per 5mL buffer) were added to each well. Plates were then allowed to develop in low light conditions for approximately 10 min, and absorbance was measured at 405 nm using an EPOCH (Biotek) plate UV/Vis spectrophotometer. Wells that indicated positive result for the presence of PLRV would become yellowed during this development period. Absorbance readings for the *N. benthamiana* tissue inoculated with PLRV infectious clones were compared to controls. Tissue infiltrated with PLRV infectious clones that were positive by DAS-ELISA and LB4404 mock infiltrated tissue that was negative for PLRV, were used for subsequent cyrogrinding and virus purification.

Cryogenic lysis of plant tissue

PLRV infected or non-infected *N. benthamiana* and systemically infected potato (*S. tuberosum*) leaf tissue was pooled and ground into a course powder in liquid nitrogen using a mortar and pestle. A moderate amount of liquid nitrogen was placed in the mortar and pestle, followed by the samples that had been kept at -80°C. Initial grinding was performed until leaf tissue was finely ground. Liquid Nitrogen was allowed to completely evaporate and tissue turned a pale green color. Samples were then quickly transferred to prelabled 50mL Falcon tubes that had been cooled in liquid nitrogen. Precautions were taken to ensure that the sample never thawed during the grinding process, as indicated by color. After the initial grinding, samples were cryogenically lysed using a mixer mill MM 400 (Retsch). Cylinders plus stainless steel balls for the MM 400 were chilled in liquid nitrogen for 30 min prior to use. Approximately 15-20 mL of tissue were placed inside the cylinders with the ball bearing, and ground for three sets

of 3 min at a frequency of 30 Hz. Between each run, the cylinders were cooled in liquid nitrogen for 5 min. After cryo-grinding, samples were transferred to new 50mL Falcon tubes pre-chilled in liquid nitrogen. For Personal protection tongs and gloves were used to handle the cylinders and samples. Spatulas used to transfer the samples were cooled in liquid nitrogen to prevent thawing of tissue.

Purification of Potato Leafroll Virus from *N. benthamiana*

PLRV purification from infiltrated tissue was performed as follows: Approximately 25-30 g of cryogenically lysed *N. benthamiana* PLRV infected leaf tissue was homogenized in 0.1M citrate buffer pH 6.5 containing 0.5% 2-mercaptoethanol (5 mL buffer per gram of tissue) using a Waring blender at 4°C. Blending was performed at low speed for 30s, high for 30s, and again low for 30s. Sides of the blenders were scraped, and samples were blended eight more times for a total of 3 sets of 3 blends total. After each set of 3 blends, a brief break was needed to ensure that samples did not warm from the heating of the blenders. Total blending time was approximately 30-40 min. Samples were then filtered through cheesecloth and accurate volume measurements were taken using graduated cylinders.

Samples were put on ice in a fume hood, and a 5% volume of 2:1 Chloroform:n-Amyl Alcohol mixture was added. Samples were covered with parafilm and allowed to stir on ice in the hood for 30 min.

Samples were then transferred into 250mL bottles and centrifuged for 10 min at 8000 rpm at 4°C in JA 14 Beckman rotor. Equal weights of water and sucrose were added to separate centrifuge bottles to act as balance.

Aqueous supernatant was recovered by aspirating, and care was taken not to also aspirate any of the liquid chloroform layer at the bottom. Supernatant was poured into graduated cylinder to measure, and then transferred to beakers. In 4°C cold room on stirrers, 0.2M NaCl and 8% PEG (final concentration) were slowly added to samples. NaCl was added first, and then PEG was added slowly by sprinkling into the mixture, stirring at low speed. After all PEG was dissolved, beakers were covered with parafilm and stirrers were slowed to lowest setting and allowed to stir overnight at 4°C.

Samples were then transferred to 250mL centrifuge bottles, and centrifuged at 8000 rpm for 20 min at 4°C in a JA 14 Beckman rotor. Supernatant was poured off and discarded, and sides of bottles were wiped down completely with Kimwipes, carefully so as to not touch the pellet. $1/10^{th}$ the original citrate buffer volume of 0.1M potassium phosphate buffer pH 7 was added to each pellet and the pellets resuspended with a rubber policemen. Partially re-suspended pellets were then transferred to glass tissue grinder and completely homogenized. Sample can stand overnight at 4°C if needed due to time constraints. Suspension was then transferred to 50mL centrifuge tubes, and spun for 10 min at 7000rpm in JA-20 rotor.

Supernatant was then saved and layered onto a 30% sucrose pad (1:4 sucrose:supernatant). Ti50.2 bottles hold a 5 mL pad plus approximately 19 mL supernatant. Sucrose was buffered in 0.1M potassium phosphate buffer. Pipettes with twisted ends were used to layer the supernatant onto the sucrose pad, as to minimize interface disturbance. Tubes must be equal weight or balanced blank counterweight tubes must be made. Samples were then centrifuged for 2 hrs at 40,000 rpm in Ti50.2 rotor, at 4°C with vacuum and maximum acceleration and maximum deceleration.

Supernatant was discarded, and tubes were again wiped with Kimwipes. Samples were covered with 0.5mL of potassium phosphate buffer, crushed with glass rods and pipetted up and down to further break up the pellets. Tubes were covered with parafilm and allowed to sit overnight at 4°C.

The supernatant was layered on top of a 10–40% linear sucrose gradient and centrifuged for 2.5 h at 111,132 g in a SW41 swinging bucket rotor (Beckman Coulter). Gradients were fractionated using a density-gradient fractionator (Teledyne-ISCO) and the virus fractions were concentrated by centrifuging for 1.5 h at 117,734 g in a Ti70 rotor (Beckman Coulter). The supernatant was discarded and the pellet was resuspended in 0.1 ml 0.1 M potassium phosphate buffer, pH 7. Virus concentration was determined by reading the A260, A280 and A320 and using the following calculation: [(A2602A320)/dilution factor]/8.0 (Takanami and Kubo 1979). Purified virus was aliquotted and stored at -80°C before use.

Microtitre Plate PLRV Co-Immunoprecipitation

Wells of microtitre plates (Agdia, Elkhart IN) were coated with a 1:200 dilution of anti-PLRV capture antibody (Agdia, Elkhart IN) in coating buffer (15 mM Na_2CO_3, 35 mM $NaHCO_3$) and incubated at 37°C for 2 hrs. Plates were washed three times with 1X phosphate-buffered saline, pH 7.2 (PBS) made with nanopure H_2O.

Plant proteins were extracted from cryo-ground mock/healthy and infected *N. benthamiana* and potato tissue by adding 500 microliters of 1X PBS buffer supplemented with Halt™ EDTA-free Protease inhibitor cocktail (1X) per 200 mg of tissue. Extracts were incubated on ice for 1 hr. Concentration of extracts was determined by a Bradford assay (Bio-Rad, Hercules CA) using bovine serum albumin as a standard and viral titer assayed by DAS-ELISA

(Lee et al, 2002). Extracts were immediately used for plate co-immunoprecipitation experiments without centrifugation. 100 ul of plant extract was added to antibody-coated wells and incubated at 4°C, overnight in a covered plastic container. Plant homogenate was carefully removed with a pipette and plates washed four times with an excess amount of 1X PBS and dried by knocking on Kimtech Science KimWipes® (Kimberly-Clark, Roswell GA). Plates were stored at –80°C until the on-plate digestion. A total of 3 technical replicates were performed for each biological replicate. One biological replicate of purified WT PLRV virus was also included. Biological replicates represent independent samples from different infected plants.

On-plate Sample Preparation For Mass Spectrometry

Protein complexes resulting from the microtitre plate Co-IP were reduced by adding 22 μL of 6M Urea, 10 mM dithiothreitol (DTT) in 100 mM ammonium bicarbonate (ABC) to each microtiter well and pipetting vigorously to re-suspend protein complexes. Plates were sonicated for 2 min and incubated at 37°C for 1 hr. Samples were alkylated with 30 mM methyl methanethiosulfonate (MMTS) in the dark for 1 hr at 37°C. Microtiter plates were sonicated for 2 min and the urea in each sample diluted to 1M with 100 mM ABC. Proteins were then digested with 100 ng of sequencing grade trypsin (Promega, Fitchburg, WI) overnight at 37°C. After digestion, plates were sonicated for 10 min and dried in speed vac. Samples were re-suspended in 20 uL of 0.1% formic acid, sonicated and desalted using C18 Zip-tips (Millipore, Billerica, MA). Peptides were stored at -80°C prior to MS analysis.

LC-MS Methods (Discovery – LTQ Orbitrap Velos)

Dried samples were reconstituted with 8 uL 3% ACN with 0.1% trifluoroacetic acid

(TFA) and splitless nanoflow chromatography was performed in the vented column configuration using a Waters NanoAcquity LC system (Waters Corporation, Milford, MA). Solvents A and B were 99.9/0.1 water/formic acid and 99.9/0.1 acetonitrile/formic acid, respectively. A flow rate of 2 μL/min (98%A/2% B) flushed sample out of a 5 μL loop and onto a self-packed capillary trap column (100 μm ID × 4 cm). After 10 μL of wash, the six port valve switched and closed the vent which initiated the gradient flow (250 nL/min) and data acquisition. A 40 min gradient was utilized in which Solvent B ramped from 2-32 % over 40 mins (1-41 min); held constant at 80% for 5 mins (41-46 mins) and initial conditions were restored for the final 14 mins (46-60 mins).

For mass spectrometric analysis an Orbitrap-Velos (ThermoFisher, Bremen Germany) was employed and operated in data dependent mode where the 10 most abundant ions were selected for tandem MS per precursor scan. For MS1 analysis performed in the orbitrap, a scan range of m/z 400-1400 with a resolving power of 60,000 @ m/z 400 was employed. Automatic gain control was set to 1,000,000 ions with a max ion injection time of 200 ms. For data dependent MS2 scans, performed in the ion trap with an AGC of 10000 ions and a max ion injection time of 80 ms. A 60s exclusion window was used to avoid repeated interrogation of abundant ions. For selection of ions, monoisotopic precursor selection (MIPS) was on with the exclusion of unassigned and 1^+ charge states.

Database Searching

For the shot-gun analysis of Co-IPs, tandem mass spectra were converted into mzXML and mascot generic format (MGF) peak list files using tools in the Trans-Proteome Pipeline (18). For *N. benthamiana* Co-IPs, an in-house protein database was created from *N. benthamiana*

protein sequences received from Greg Martin (BTI). Potato Co-IPs were analyzed using an in-house database created using amino acid sequences corresponding to all coding gene sequences of *S. tuberosum* Group Phureja DM1-3 516R44 (CIP801092), International Potato Genome Sequencing Consortium (PGSC) genome annotation v3.4, downloaded from the Solanaceae Genomics Resource website at Michigan State University (http://solanaceae.plantbiology.msu.edu/index.shtml). Both plant databases contained luteovirus and common Co-IP contaminant sequences obtained from NCBI. All data were searched using Mascot v2.3.02 (Matrix Science, Boston, Ma) as follows. Fixed methylthio and variable methionine oxidation were used as modifications. Precursor ion tolerances were set at 30 ppms and fragment tolerance was 0.8 Daltons. The enzyme selected was trypsin with 1 missed cleavage permitted. A scrambled decoy database was used to search for calculating a false discovery rate.

Mascot *.dat files were created from the co-IP and control search results and loaded into Scaffold (version 3_00_05). Search parameters were the same as for Mascot including the in-house protein databases used. We reported protein accession numbers that could be identified on the basis of at least one peptide with a Mascot score exceeding the identity threshold and E-value <0.05. The probability threshold for protein identification was selected empirically to maintain a false-discovery rate of less than 1.0%. Spectral counts were normalized to the total. Normalized spectral counts for each peptide identified were compared between co-IP and control experiments, and a Student's T-test was performed. Proteins detected in both the co-IP and control are only reported if they had greater than a 2.5-fold enrichment in the co-IP, $p<0.05$. Fold change calculations were performed by dividing spectral counts of proteins for comparison between strains. These data were reported in log base 2 form, such that a fold change of 2 is

equal to a log base 2 fold change of 1. All those positive log base 2 fold changes indicate enrichment in the respective strain of interest, negative log2 values indicate enrichment of the opposing strain, and log base 2 fold change equal to 0 represents no change in spectral counts between compared strains. Binning and histograms were constructed utilizing Excel v.14.3.2, and bin limits were selected based on the distribution of data.

Results

An improved workflow for the identification of virus-interacting plant proteins.

PLRV's coat and readthrough proteins can be seen as the purple and grey regions in the proposed schematic of the virus (Fig.1), respectively. LC-MS/MS analysis of virus purified from *Agrobacterium*-infiltrated *N. benthamiana* leaves resulted in only 18% peptide coverage of the RTP with no peptides from the C-terminal region being identified (Fig.2B). These data are consistent with Western blot analysis of purified PLRV in which only a truncated version of the RTP was detected using antibodies against the CP domain (Peter et al. 2008), suggesting that the C-terminal domain of the RTP is somehow truncated during the purification process. In contrast to the analysis of purified virus, the co-IP method (Fig.3) resulted in a higher percent coverage of the RTP (36%) and peptides from the C-terminal region could be detected (Fig.2C). Thus, it appears that the co-IP may enables a more gentle isolation of virus that preserves the C-terminal domain and putative interactions with the host proteins interacting with this region of the virus.

Nicotiana benthamiana as a model system to study PLRV-plant protein interactions.

A total of 721 proteins were identified using the co-IP method. These proteins can be divided between two groups: those found in both the mock infiltrated and the wild type (WT)

PLRV co-IP reactions and those specific only to the WT co-IP reactions. There were 678 proteins found in both mock infiltrated and the WT, and 26 proteins were detected only in the WT infected tissue Co-IP (Table 1). Many of the proteins had spectral counts less than 5. While these are not ideal for quantification using spectral counting, these were reported here for completeness of the dataset. Proteins with very few spectral counts are likely to be low abundant proteins and not adequately sampled using data dependent LC-MS/MS. With very few spectral counts, it is difficult to discern whether these are meaningful differences between the experiments or differences in the mass spectrometric analysis.

Of those 678 proteins found in both WT and mock LB4404, levels of enrichment from mock LB4404 to WT PLRV varied considerably (Fig.4A). Many proteins were not significantly enriched in WT PLRV, with 324 having a fold change less than 1, p value > 0.05. There were 48 proteins that had the same spectral counts between WT PLRV and mock, and so had a fold change equal to 1, and therefore a $\log_2$(fold change) of 0 (Fig.4A). The remaining proteins were enriched in WT PLRV over mock, with 306 proteins having an enrichment in WT PLRV greater than 1-fold. Among these proteins, 241 were between 0 and 1 $\log_2$(fold change), 49 were between 1 and 2, 14 were between 2 and 4, and finally 2 proteins were between 4 and 6 $\log_2$(fold change) enrichment.

There were a total of 25 proteins found to be unique to WT PLRV infected Co-IP samples that were not detected in the mock Co-IP. Importantly, the protein that showed the most enrichment in the WT co-IP reaction was the PLRV CP-RPT with a spectral count of 315. Of the remaining proteins, 16 had spectral counts below 10 in WT PLRV, while 7 had between 10 and 50 spectral counts. The second and third most enriched proteins, with a spectral counts of 112 and 58 respectively, were identified as class 1 heat shock proteins (Table 1).

Using molecular virology to define domains of interaction between virus and host proteins

To identify host proteins that may be interacting with the RTP, we inoculated *N. benthamiana* leaves with a PLRV infectious clone that does not express the RTP (Peter et al. 2008) and compared plant proteins co-immunoprecipitating with mutant virus to those we identified co-immunoprecipitating with WT PLRV. Consistent with the fact that the mutant fails to express the RTP, we could not detect any peptides from the RTD domain (Fig.2D). By comparing data from co-IP analysis of WT PLRV and the ΔRTP mutant, we identified proteins that are specific to the CP or RTP respectively. A total of 704 proteins were found in WT PLRV, 38 of which were not detected in ΔRTP co-IP. Of those 38 proteins, 18 were enriched over mock, and 5 were not detected in mock LB4404 at all (Table 2). Fold changes between the WT and ΔRTP co-IPs can be seen in Fig.4B. A total of 133 proteins had a fold change less than one, meaning they had higher spectral counts in the ΔRTP mutant as opposed to WT PLRV. The remaining proteins were enriched in WT compared to ΔRTP, with 381 having greater than 1-fold change, 104>2-fold, 8>4-fold, and 4>10-fold. Those proteins found co-immunoprecipitating with WT PLRV and not the ΔRTP mutant are of particular interest as they may represent proteins that play a role in facilitating systemic movement of the virus and/or phloem retention of the virus, both of which are mediated by the domains of the RTP.

Moving into a natural host of PLRV we co-immunoprecipitated WT virus from systemically infected potato plants and compared the presence of those proteins we found to co-IP with WT virus in *N. benthamiana*. Of those 306 proteins present in both WT PLRV and mock, and enriched in WT PLRV co-IP over mock-infiltrated *N. benthamiana,* 7 were also detected in the WT PLRV co-IP from potato (Table 3). Interestingly, spectra derived from four of these

proteins were not detected in the co-IP of the ΔRTP mutant in *N. benthamiana* and were only detected in the experiments with WT virus in *N. benthamiana* and systemically infected potato (Table 3).

Discussion

The C-terminal region of the virus plays a major role in the restricted movement of PLRV and thus is an important domain for the identification of virus-plant protein interactions mediating phloem retention and systemic infection in plants. Traditionally, plant viruses are purified from the sap using density gradient centrifugation (Rochow and Brakke 1964). Our originally proposed workflow to identify host proteins in complex with PLRV purified from infected *N. benthamiana* proved to be too harsh to be useful for our intended analysis. Peptides from the C-terminal region of the RTP could not be detected by LC-MS/MS analysis of purified WT PLRV (Fig.2B), suggesting a co-analytical modification of the RTP resulting in removal of the C-terminal domain during the purification process. These data are consistent with the fact that only a truncated RTP can be detected by Western analysis of purified PLRV using antibodies specific to the N-terminal region of the CP (Peter et al. 2008). In contrast, a co-IP workflow enabled us to isolate virions with the full length RTP (Fig.2C) directly from infected tissue homogenate with no clearing in organic solvents or precipitation using polyethylene glycol. Following co-IP, peptides derived from the C-terminus of the RTP were consistently detected by LC-MS/MS analysis. Thus, these data show that the co-IP method was likely better suited also to identifying plant proteins interacting with the C-terminal domain of the RTP and functionally involved in retaining the virus within the phloem. The complement of host plant

proteins found to interact with PLRV, either directly or in complex, is referred to here as the interactome.

Comparison of proteins co-immunoprecipitating with PLRV from infected *N. benthamiana* to the mock-infiltrated controls enabled us to identify 25 proteins in complex with the virus capsid and not detected in the control reactions. These 25 proteins comprise the first description of the PLRV-plant protein interactome and reveal how the virus may usurp existing transport pathways in plants for cell-to-cell and systemic movement. PLRV moves from cell-to-cell as a virion that is a protein capsid encasing the viral genome. In plants, plasmodesmata are small membrane lined channels that provide cytoplasmic connectivity among plant cells (Cilia and Jackson 2004). PLRV moves from cell-to-cell through plasmodesmata. Hence, we hypothesized that proteins interacting with PLRV discovered in our experiment may be components of the plasmodesmata. Comparison of the proteins found in the PLRV-plant protein interactome to those described in the plasmadesmata proteome of *Arabidopsis thaliana* (Fernandez-Calvino et al. 2011)reveals that there is a 12.37% overlap in the proteins may prove to relate to cell-to-cell communication in plants, a key aspect of virus transmission. *Arabidopsis* is not a natural host of PLRV, although our preliminary data indicates that the model plant does support PLRV replication and virion formation (not shown). *Arabidopsis* may be a good model plant to test the functions and subcellular localization, as many genetic tools are available for these types of analyses in *Arabidopsis.*

The RTP is exposed on the surface of PLRV virions (Chavez et al. 2012). The exposed surfaces on the virion can function in virus-plant protein interactions. A mutant of PLRV that does not express the C-terminal domain of the RTP is not retained in phloem tissue. The virus is detected in surrounding mesophyll tissue (Peter et al. 2009). Furthermore the sub-cellular

481 localization of the mutant virus is changed from cytoplasmic to chloroplasmic membranes (Peter
482 et al. 2009). We hypothesize that these phenotypic changes of the virus are due to changes in
483 how the mutant virus, lacking the C-terminal domain of the RTP, interacts with various plant
484 proteins. To test this hypothesis, we performed co-IP with a virus mutant that does not express
485 the RTP. The hypothesis being that plant proteins interacting with the CP component of the
486 virion will still be detected but plant proteins that interact with the RTP will not. This
487 comparison enabled us to map where these protein interactions are occurring on the surface of
488 the virus. Therefore, those proteins uniquely co-immunoprecipitating with WT PLRV, and not
489 enriched in analysis of either mock or mutant, are of particular interest to our study as they
490 represent those plant proteins interacting with the RTP and are candidates for restricting virus
491 movement within the plant. Furthermore, comparison of the interactomes between the model
492 plant *N. benthamiana* and the natural host potato enabled us to understand how the virus
493 functions in both systems and the best protein candidates to pursue for functional studies in
494 future work.

495 Four proteins were found matching the following criteria, greater than 2.5-fold
496 enrichment of spectral counts for WT PLRV as compared to mutant and mock infected *N.*
497 *benthamiana* and are also greater than 2.5-fold enriched in WT PLRV infected potato over
498 healthy potato (Table 3). These four proteins include 14-3-3 protein (AT1G78300.1), elicitor-
499 inducible protein EIG-J7, membrane steroid-binding protein 2, and probable 26S proteasome
500 non-ATPase regulatory subunit 3. Queries for studies of the functions of these protein families
501 yield promising results. Within the family of 14-3-3 proteins in *N. benthamiana* and in other
502 systems (Oh et al. 2010; Oh and Martin 2011), 14-3-3 proteins are involved in plant immunity,
503 signal transduction pathways to trigger plant immunity, as well as regulating immunity-

associated programmed cell death pathways. Our finding that certain 14-3-3 proteins co-precipitate with PLRV is encouraging, and indicative that PLRV may disrupt these important pathways to prevent plant immunity and promote plant infection. Regarding the elicitor-inducible protein EIG-J7, a study by Takemoto and colleagues found that these proteins have roles in activation of plant disease resistance and stress responses (Takemoto et al. 2001). PLRV may interact with EIG-J7 to activate pathways that help overcome resistance and modulate stress responses. These interactions make sub-cellular conditions favorable for virus replication or systemic movement. An interaction between PLRV and the membrane-steroid binding protein also reveals that PLRV is hijacking cellular pathways that are crucial for plant development. Membrane-steroid binding proteins enhance vesicle trafficking necessary for auxin redistribution so that plants can respond to gravity (Yang et al. 2008). Our finding of this protein suggests that PLRV may utilize vesicles to move within the plant, as it is known to do within its aphid vector (Gray and Gildow 2003). Membrane steroid binding protein is also a key regulator of cell elongation (Yang et al. 2005). An interaction between PLRV and membrane steroid binding protein indicates that the virus has evolved to use pathways in plants that are critical for plant development and survival. Most interestingly, membrane steroid binding protein also negatively regulates brassinosteroid signaling (Song et al. 2009), a key pathway involved in plant herbivory. These data indicate that PLRV may also make conditions favorable for aphids to feed and acquire virus. Regarding the final protein of interest, 26S proteasome subunit 3, it was found by Jin and colleagues that RPN9 within this family of 26S proteasome subunit proteins is involved with broad-spectrum virus systemic transport within the vascular system of *N. benthamiana.* These researchers also found that RPN9 functions in part through regulation of auxin transport, similar to membrane-steroid proteins discussed previously (Jin et al. 2006). An interaction

between RPN9 and PLRV suggests that PLRV may use this protein for improved viral systemic movement throughout the vascular system of the plant. The focus of future studies will be to validate a direct interaction between these proteins and PLRV and to define the function of these plant proteins in PLRV infection.

Conclusion

Our work has yielded a list of candidate proteins interacting with PLRV, but future work still remains to validate our results and to further identify those proteins specifically interacting with the C-terminus of PLRV's RTD. Fluorescent tagging, co-localization, and additional studies with additional mutants will allow validation of our results. Analysis of mutants with partial deletion of the RTP, such as the SYG mutant that has deletion of only the C-terminal domain of the RTD, would be the next step for this work. Comparison of proteins co-immunoprecipitating with the SYG mutant would allow us to narrow the list of proteins to those interacting with the C-terminal domain and thus more likely to be involved in restricting virus movement within the phloem plant.

Eventually, it is hoped that this expansion of proteomic knowledge of PLRV's plant protein interactions will yield improved methods for virus disruption. With increasing understanding of how PLRV interacts with plant proteins, it will be possible to develop virus management strategies that target the virus and the aphid vector. Conventional methods for controlling PLRV involve the use of prophylactic insecticides, which may have dangers due to its non-specificity and possible human health risks. The alternative of virus disruption at the site of plant interaction should be pursued through validation and continuation of this research.

Figure Legends

Fig. 1 Simulated visualization of PLRV capsid
Purple regions represent the coat protein (CP), grey regions represent the readthrough protein (RTP). This is a model of what we hypothesize the structure to look like although no structural data are available for any luteovirid yet.

Fig. 2 Readthrough protein peptides detected by LC MS/MS analysis of PLRV Co-immunoprecipitations A. The functional domains of the RTP of PLRV purple indicating the domain coding for the CP, and grey indicating the readthrough domain of the RTP. Peptides detected in the analysis of **B.** sucrose-gradient purified PLRV, **C.** WT PLRV co-immunoprecipitated from *N. benthamiana* and **D.** ΔRTP mutant co-immunoprecipitation. Yellow and green strips indicate the position of the modified and un-modified peptides detected along the region of the RTP, respectively.

Fig. 3 Co-immunoprecipitation workflow A. Extracting virus-plant protein complexes. *N. benthamiana* agro-infiltrated leaf tissue is collected and cryogenically lysed (right). Proteins complexes were extracted using a non-detergent buffer supplemented with protease inhibitors. **B.** Immunoprecipitation of complexes. Plant homogenate is applied to a 96-well plate coated with an anti-PLRV antibody (Agdia), then loaded with the samples (right). Plates are then incubated and washed with buffer to remove unbound host proteins and minimize unspecific protein interactions. **C.** LC MS/MS analysis. Virion-plant protein complexes are reduced, alkylated and hydrolyzed into peptides using the enzyme trypsin in the wells of the plate. Resulting peptides are analyzed using a mass spectrometer. **D.** Data analysis. Proteins were identified by database searching using Mascot and label-free quantification was performed using Scaffold.

Fig. 4 Fold Enrichment Histogram of plant peptides identified in PLRV co-immunoprecipitations from *N. benthamiana* Histograms of the log base 2 of the fold change of combined peptide spectral counts for proteins identified in **A.** mock-infiltrated to WT PLRV co-IP, and **B**. ΔRTP mutant to WT PLRV co-IP with x-axis showing the ranges of the magnitude of fold changes, 0 includes all those negative fold changes less than or equaling zero, 1 includes all those from 0 less than or equal to 1, etc. Fold changes less than 0 indicate that the peptide had higher spectral counts in mock or ΔRTP mutant co-IP compared to the WT PLRV co-IP, whereas fold changes greater than 0 indicate enrichment in WT PLRV. Fold changes equal to 0 indicate equal spectral counts in both mock LB4404 and WT PLRV. Height of the bar represents the frequency, or the numbers of proteins found to have that level of enrichment of spectral counts from mock to WT PLRV. **B.** Histogram of the log base 2 of the change from ΔRTP mutant to WT PLRV, with x-axis showing the ranges of the magnitude of fold changes from ΔRTP to WT PLRV; 0 includes all those negative fold changes less than or equaling zero, 1 includes all those from 0 less than or equal to 1, etc. Fold changes less than 0 indicate that the peptide had higher spectral counts in ΔRTP mutant than WT PLRV, whereas fold changes greater than 0 indicate enrichment in WT PLRV over mutant. Fold changes equal to 0 indicate equal spectral counts in both mutant and WT PLRV. Height of the bar represents the frequency, or the numbers of proteins found to have that level of enrichment of spectral counts from ΔRTP mutant to WT PLRV.

Fig. 1

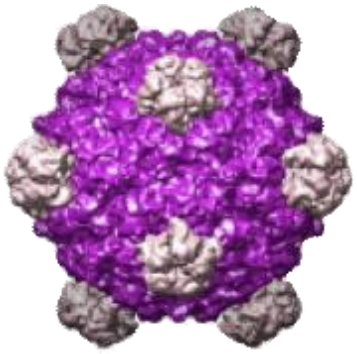

Fig. 2

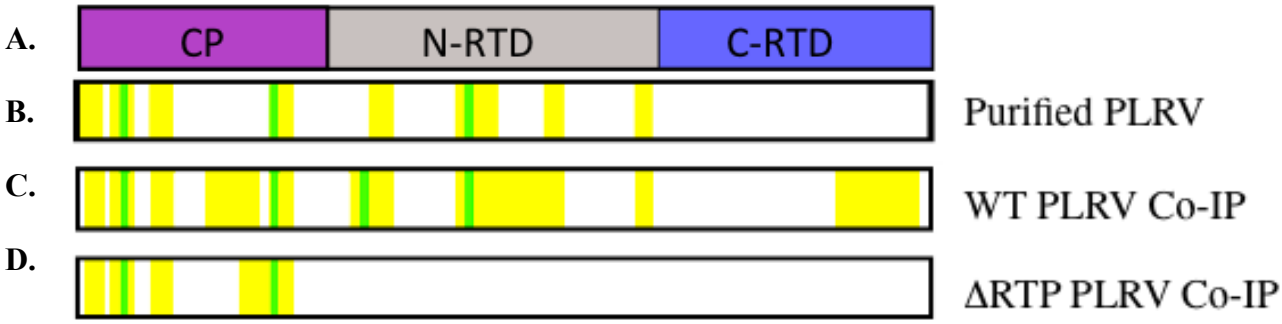

Fig. 3

A.

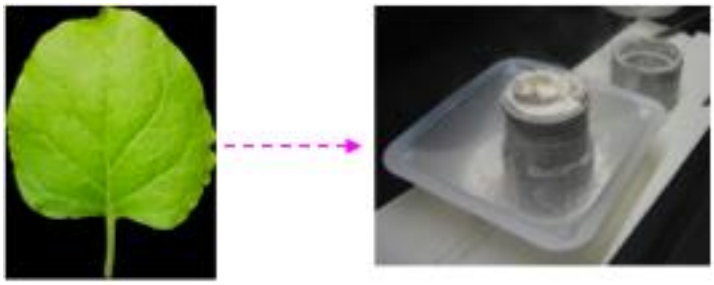

B.

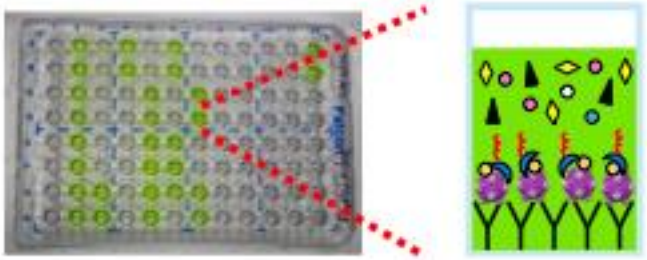

C.

D.

Fig. 4

A.

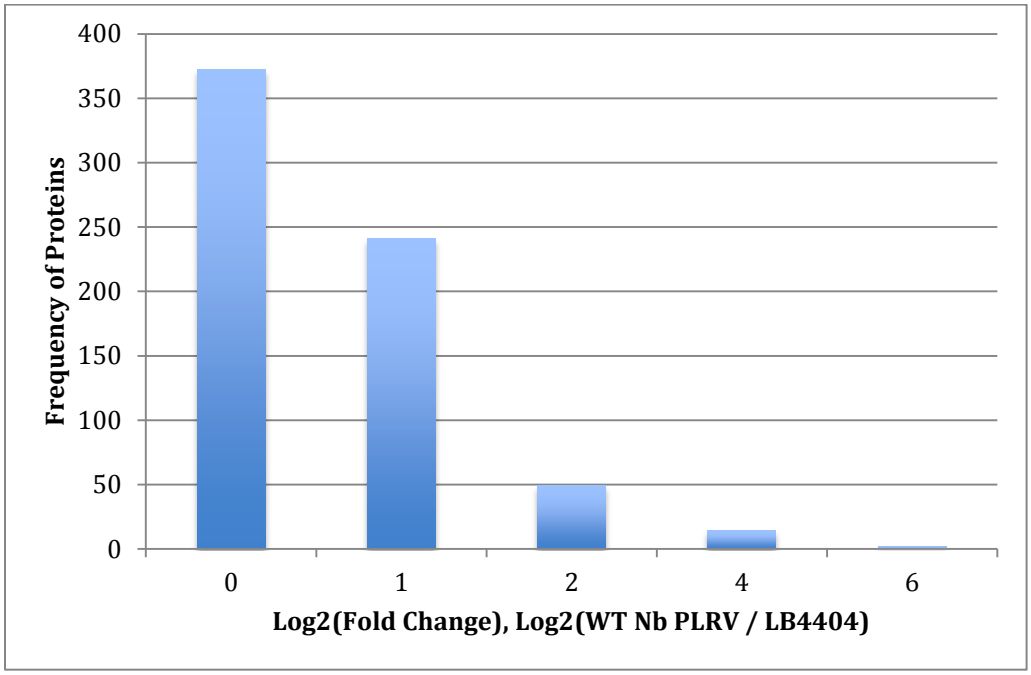
Frequency of Proteins
400
350
300
250
200
150
100
50
0
0
1
2
4
6
Log2(Fold Change), Log2(WT Nb PLRV / LB4404)

B.

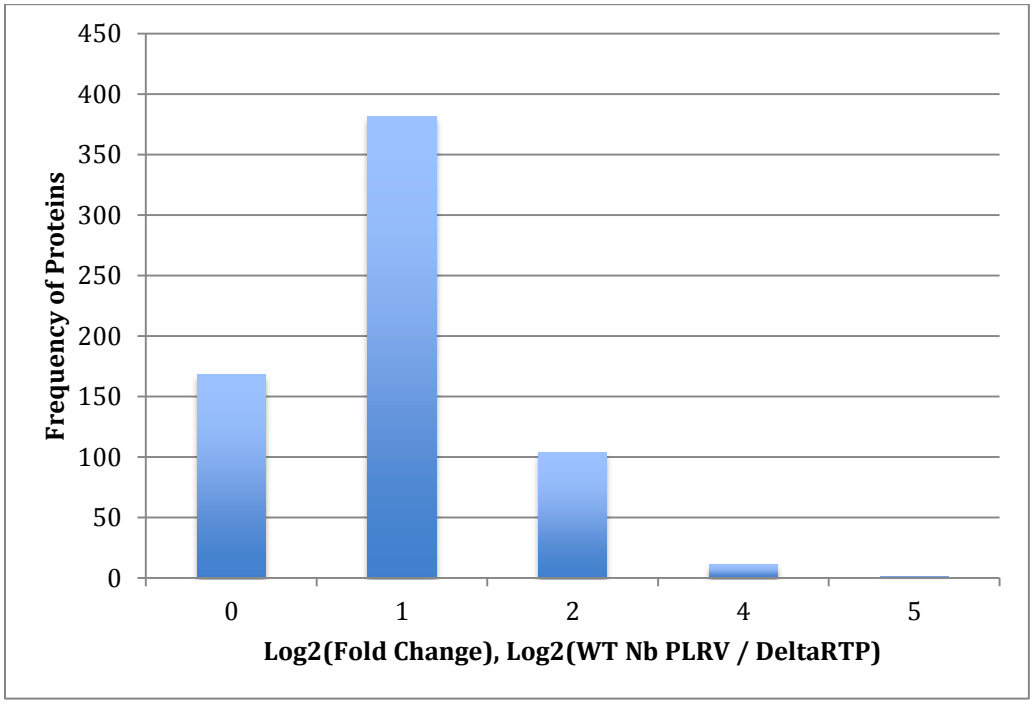
Frequency of Proteins
450
400
350
300
250
200
150
100
50
0
0
1
2
4
5
Log2(Fold Change), Log2(WT Nb PLRV / DeltaRTP)

Table 1: 25 proteins detected only in Wild Type *Potato leafroll virus* co-immunoprecipitation of *N. benthamiana*, not found in mock LB4404 *N. benthamiana.*

#	Common name, if available[a]	Accession Number[b]	Spectral Counts		
			LB4404	ΔRTP	WT PLRV
1	Dynamin-related protein 1E	NbS00056353g0008.1	0	1	1
2	Alanine aminotransferase 2, mitochondrial	NbS00001174g0003.1	0	7	2
3	Uncharacterized isomerase BH0283	NbS00013552g0018.1	0	7	2
4	Probable signal peptidase complex subunit 2	NbS00035415g0012.1	0	0	2
5	Succinate-semialdehyde dehydrogenase, mitochondrial	NbS00016765g0002.1	0	5	2
6	Benzyl alcohol O-benzoyltransferase	NbS00053630g0004.1	0	0	3
7	Hypersensitive-induced response protein 1	NbS00010140g0005.1	0	3	4
8	Importin subunit alpha-1b	NbS00022414g0008.1	0	0	4
9	Probable carboxylesterase 17	NbS00031166g0001.1	0	7	4
10	Citrate synthase 2, peroxisomal	NbS00001219g0008.1	0	6	5
11	Auxin-induced in root cultures protein 12	NbS00002670g0023.1	0	2	5
12	Aldehyde dehydrogenase family 2 member B7, mitochondrial	NbS00023446g0007.1	0	8	5
13	Probable mitochondrial-processing peptidase subunit beta	NbS00030413g0012.1	0	4	6
14	P1 protein [Potato leafroll virus]	gi|9629162|ref|NP_056747.1|	0	18	8
15	Probable pyridoxal biosynthesis protein PDX1.2	NbS00004324g0003.1	0	17	8
16	UDP-glucose flavonoid 3-O-glucosyltransferase 7	NbS00038176g0004.1	0	6	12
17	14-3-3-like protein B	NbS00007737g0010.1	0	0	12
18	3-ketoacyl-CoA thiolase 2, peroxisomal	NbS00006179g0007.1	0	19	13
19	22.0 kDa class IV heat shock protein	NbS00027674g0005.1	0	20	16
20	Vetispiradiene synthase 1	NbS00023487g0001.1	0	14	18
21	5-epi-aristolochene synthase 2	NbS00055581g0001.1	0	10	20
22	putative genome-linked protein [Potato leafroll virus]	gi|9629165|ref|NP_056750.1|	0	14	49
23	17.6 kDa class I heat shock protein 3	NbS00041882g0003.1	0	90	58
24	17.6 kDa class I heat shock protein	NbS00025860g0007.1	0	111	112
25	CP read-through protein [Potato leafroll virus]	gi|21040163|ref|NP_056751.2|	0	136	315

[a]Top hit by NCBI BLAST p
[b]accession number in *N. benthamiana* database if available

751 **Table 2:** 38 Proteins found in Wild Type *Potato leafroll virus* infected *N. benthamiana* co-
752 immunoprecipitation samples that were not detected in mutant ΔRTP.

			Spectral Counts	
#	Common Name (if available)[a]	Accession Number[b]	WT PLRV	ΔRTP
1	unknown	NbS00016243g0202.1	14	0
2	unknown	NbS00028158g0015.1	13	0
3	PREDICTED: cell division protein ftsY homolog	NbS00043750g0009.1	13	0
4	14-3-3 protein	NbS00007737g0010.1	12	0
5	elicitor-inducible protein EIG-J7	NbS00000603g0001.1	11	0
6	Probable 26S proteasome non-ATPase regulatory subunit 3	NbS00022314g0010.1	7	0
7	Eukaryotic translation initiation factor 3 subunit A	NbS00047179g0008.1	7	0
8	PREDICTED: importin-5	NbS00021039g0022.1	7	0
9	ADP-glucose pyrophosphorylase large subunit	NbS00050736g0008.1	7	0
10	PREDICTED: DEAD-box ATP-dependent RNA helicase 3, chloroplastic	NbS00021398g0012.1	7	0
11	unknown	NbS00019281g0111.1	6	0
12	ATP-dependent transporter, putative	NbS00027404g0011.1	6	0
13	steroid binding protein, putative	NbS00002963g0012.1	5	0
14	PREDICTED: 30S ribosomal protein S13, chloroplastic	NbS00015597g0013.1	5	0
15	NADH dehydrogenase	NbS00037482g0007.1	5	0
16	hypothetical protein VITISV_006765	NbS00002677g0011.1	5	0
17	PREDICTED: protein TIC110, chloroplastic-like	NbS00009678g0004.1	5	0
18	Impa2	NbS00022414g0008.1	4	0
19	PREDICTED: eukaryotic translation initiation factor 3 subunit E-like	NbS00019594g0006.1	4	0
20	(3R)-hydroxymyristoyl-[acyl-carrier-protein] dehydratase	NbS00001520g0010.1	4	0
21	mitochondrial carrier protein	NbS00040758g0005.1	4	0
22	Long chain acyl-CoA synthetase 1	NbS00003746g0008.1	4	0
23	calcium homeostasis regulator CHoR1	NbS00016355g0014.1	4	0
24	hsr201	NbS00053630g0004.1	3	0
25	unknown	NbS00002820g0009.1	3	0
26	PREDICTED: uncharacterized protein LOC100817904	NbS00009423g0004.1	3	0
27	PREDICTED: protein TIC 55, chloroplastic-like	NbS00029739g0004.1	3	0
28	Aquaporin PIP2.2, putative	NbS00017323g0009.1	3	0
29	unknown	NbS00012711g0115.1	3	0
30	Isocitrate dehydrogenase [NADP], chloroplastic (Fragment)	NbS00023296g0014.1	3	0
31	hypothetical protein ARALYDRAFT_483034	NbS00035415g0012.1	2	0
32	unknown	NbS00037340g0107.1	2	0
33	Translation factor GUF1 homolog, chloroplastic	NbS00020149g0020.1	2	0
34	Uncharacterized methyltransferase At2g41040, chloroplastic	NbS00036203g0005.1	2	0
35	RNA binding protein, putative	NbS00010360g0002.1	1	0
36	sexual organ expressed protein	NbC24872723g0001.1	1	0
37	Protein ASPARTIC PROTEASE IN GUARD CELL 2	NbS00006168g0008.1	1	0
38	sulfate adenylyltransferase	NbS00024811g0011.1	1	0

[a]Top hit by NCBI BLAST p
[b]Accession number in *N. benthamiana* database

Table 3: 24 Proteins found enriched in Wild Type *Potato leafroll virus* infected *N. benthamiana*, with potato data shown

		Spectral Counts				
		N. benthamiana			Potato	
#	Protein	Mock LB4404 (13 reps)	ΔRTP (9 reps)	WT (10 reps)	Healthy Potato (9 reps)	Infected Potato (8 reps)
1	CP read-through protein	0	95	238	1	47
2[ab]	14-3-3 protein (AT1G78300.1)	0	0	10	0	9
3	Importin subunit alpha-1b	0	0	1	-	-
4	Benzyl alcohol O-benzoyltransferase	0	0	3	-	-
5	Probable signal peptidase complex subunit 2	0	0	1	-	-
6	60S ribosomal protein L18a	0	0	1	-	-
7[ab]	Probable 26S proteasome non-ATPase regulatory subunit 3	0	0	5	1	5
8[a]	heme-binding-like protein	0	0	1	12	29
9	14-3-3 protein (AT2G42590.2)	0	1	10	-	-
10	Eukaryotic translation initiation factor 3 subunit A	1	0	5	-	-
11	Importin-5	1	0	4	-	-
12[ab]	Membrane steroid-binding protein 2	2	0	5	0	5
13	ABC transporter F family member 1	2	0	6	-	-
14[ab]	elicitor-inducible protein EIG-J7	3	0	10	0	13
15	unknown protein	4	0	12	-	-
16	mitochondrial NAD-dependent malate dehydrogenase	2	3	21	-	-
17	Importin subunit beta-1	3	0	8	-	-
18	unknown protein	4	1	9	-	-
19	26S proteasome AAA-ATPase subunit RPT4a	4	1	11	-	-
20	G-protein beta subunit like	8	1	24	-	-
21	ADP-ribosylation factor GTPase-activating protein	6	5	20	-	-
22	Heat shock 70 kDa protein	10	10	32	-	-
23[a]	delta 1-pyrroline-5-carboxylate synthetase	12	8	25	0	26
24[a]	Annexin D1	15	16	36	2	17

[a]Same exact proteins found enriched in PLRV co-IP

[b]Proteins having greater than 2.5-fold enrichment in WT PLRV over ΔRTP or mock, and greater than 2.5-fold enrichment in Infected Potato over Healthy Potato

References

Bahner, I., J. Lamb, M. A. Mayo and R. T. Hay (1990). "Expression of the genome of potato leafroll virus: readthrough of the coat protein termination codon in vivo." J Gen Virol **71 (Pt 10)**: 2251-2256.

Benitez-Alfonso, Y., C. Faulkner, C. Ritzenthaler and A. J. Maule (2010). "Plasmodesmata: gateways to local and systemic virus infection." Mol Plant Microbe Interact **23**(11): 1403-1412.

Burch-Smith, T. M., S. Stonebloom, M. Xu and P. C. Zambryski (2011). "Plasmodesmata during development: re-examination of the importance of primary, secondary, and branched plasmodesmata structure versus function." Protoplasma **248**(1): 61-74.

Burch-Smith, T. M. and P. C. Zambryski (2012). "Plasmodesmata paradigm shift: regulation from without versus within." Annu Rev Plant Biol **63**: 239-260.

Chavez, J. D., M. Cilia, C. R. Weisbrod, H. J. Ju, J. K. Eng, S. M. Gray and J. E. Bruce (2012). "Cross-linking measurements of the Potato leafroll virus reveal protein interaction topologies required for virion stability, aphid transmission, and virus-plant interactions." J Proteome Res **11**(5): 2968-2981.

Chay, C. A., U. B. Gunasinge, S. P. Dinesh-Kumar, W. A. Miller and S. M. Gray (1996). "Aphid transmission and systemic plant infection determinants of barley yellow dwarf luteovirus-PAV are contained in the coat protein readthrough domain and 17-kDa protein, respectively." Virology **219**(1): 57-65.

Cilia, M., L. Cantrill and A. van Bel (2002). "Plasmodesma 2001: on safari through the symplast." Plant Cell **14**(1): 7-10.

Cilia, M. L. and D. Jackson (2004). "Plasmodesmata form and function." Curr Opin Cell Biol **16**(5): 500-506.

Cristea, I. M. and B. T. Chait (2011) "Affinity purification of protein complexes." Cold Spring Harb Protoc **2011** DOI: 2011/5/pdb.prot5611

Fernandez-Calvino, L., C. Faulkner, J. Walshaw, G. Saalbach, E. Bayer, Y. Benitez-Alfonso and A. Maule (2011). "Arabidopsis plasmodesmal proteome." PLoS One **6**(4): e18880.

Gray, S. and F. E. Gildow (2003). "Luteovirus-aphid interactions." Annu Rev Phytopathol **41**: 539-566.

Gray, S. M. and N. Banerjee (1999). "Mechanisms of arthropod transmission of plant and animal viruses." Microbiol Mol Biol Rev **63**(1): 128-148.

Jin, H., S. Li and A. Villegas, Jr. (2006). "Down-regulation of the 26S proteasome subunit RPN9 inhibits viral systemic transport and alters plant vascular development." Plant Physiol **142**(2): 651-661.

Kaplan, I. B., L. Lee, D. R. Ripoll, P. Palukaitis, F. Gildow and S. M. Gray (2007). "Point mutations in the potato leafroll virus major capsid protein alter virion stability and aphid transmission." J Gen Virol **88**(Pt 6): 1821-1830.

Liu, C. and R. S. Nelson (2013). "The cell biology of Tobacco mosaic virus replication and movement." Front Plant Sci **4**: 12.

Marin-Gonzalez, E. and P. Suarez-Lopez (2012). ""And yet it moves": cell-to-cell and long-distance signaling by plant microRNAs." Plant Sci **196**: 18-30.

Maule, A. J., Y. Benitez-Alfonso and C. Faulkner (2011). "Plasmodesmata - membrane tunnels with attitude." Curr Opin Plant Biol **14**(6): 683-690.

Mohan, B. R., S. P. Dinesh-Kumar and W. A. Miller (1995). "Genes and cis-acting sequences involved in replication of barley yellow dwarf virus-PAV RNA." Virology **212**(1): 186-195.

Oh, C. S. and G. B. Martin (2011). "Tomato 14-3-3 protein TFT7 interacts with a MAP kinase kinase to regulate immunity-associated programmed cell death mediated by diverse disease resistance proteins." J Biol Chem **286**(16): 14129-14136.

Oh, C. S., K. F. Pedley and G. B. Martin (2010). "Tomato 14-3-3 protein 7 positively regulates immunity-associated programmed cell death by enhancing protein abundance and signaling ability of MAPKKK {alpha}." Plant Cell **22**(1): 260-272.

Peter, K. A., F. Gildow, P. Palukaitis and S. M. Gray (2009). "The C terminus of the polerovirus p5 readthrough domain limits virus infection to the phloem." J Virol **83**(11): 5419-5429.

Peter, K. A., D. Liang, P. Palukaitis and S. M. Gray (2008). "Small deletions in the potato leafroll virus readthrough protein affect particle morphology, aphid transmission, virus movement and accumulation." J Gen Virol **89**(Pt 8): 2037-2045.

Ritzenthaler, C. (2011). "Parallels and distinctions in the direct cell-to-cell spread of the plant and animal viruses." Curr Opin Virol **1**(5): 403-409.

Rochow, W. F. and M. K. Brakke (1964). "Purification of Barley Yellow Dwarf Virus." Virology **24**: 310-322.

Schoelz, J. E., P. A. Harries and R. S. Nelson (2011). "Intracellular transport of plant viruses: finding the door out of the cell." Mol Plant **4**(5): 813-831.

Song, L., Q. M. Shi, X. H. Yang, Z. H. Xu and H. W. Xue (2009). "Membrane steroid-binding protein 1 (MSBP1) negatively regulates brassinosteroid signaling by enhancing the endocytosis of BAK1." Cell Res **19**(7): 864-876.

Takanami, Y. and S. Kubo (1979). "Enzyme assisted purification of two phloem-limited plant viruses." J. Gen. Virol. **44**: 153-159.

Takemoto, D., N. Doke and K. Kawakita (2001). "Characterization of Elicitor-inducible Tobacco Genes Isolated by Differential Hybridization." J. Gen. Plant Path **67**: 89-96.

Ueki, S. and V. Citovsky (2011). "To gate, or not to gate: regulatory mechanisms for intercellular protein transport and virus movement in plants." Mol Plant **4**(5): 782-793.

Yang, X., L. Song and H. W. Xue (2008). "Membrane steroid binding protein 1 (MSBP1) stimulates tropism by regulating vesicle trafficking and auxin redistribution." Mol Plant **1**(6): 1077-1087.

Yang, X. H., Z. H. Xu and H. W. Xue (2005). "Arabidopsis membrane steroid binding protein 1 is involved in inhibition of cell elongation." Plant Cell **17**(1): 116-131.